Role of Equilibrium Fluctuations in Light-Induced Order

Alfred Zong,[1,2,*] Pavel E. Dolgirev,[3,*] Anshul Kogar,[1,4,*] Yifan Su,[1] Xiaozhe Shen,[5] Joshua A. W. Straquadine,[6,7,8] Xirui Wang,[1] Duan Luo,[5] Michael E. Kozina,[5] Alexander H. Reid,[5] Renkai Li,[5] Jie Yang,[5] Stephen P. Weathersby,[5] Suji Park,[5,9] Edbert J. Sie,[7,8] Pablo Jarillo-Herrero,[1] Ian R. Fisher,[6,7,8] Xijie Wang,[5] Eugene Demler,[3,10] and Nuh Gedik[1,†]

[1]*Department of Physics, Massachusetts Institute of Technology, Cambridge, Massachusetts 02139, USA*
[2]*Department of Chemistry, University of California at Berkeley, Berkeley, California 94720, USA*
[3]*Department of Physics, Harvard University, Cambridge, Massachusetts 02138, USA*
[4]*Department of Physics and Astronomy, University of California at Los Angeles, Los Angeles, California 90095, USA*
[5]*SLAC National Accelerator Laboratory, Menlo Park, California 94025, USA*
[6]*Department of Applied Physics, Stanford University, Stanford, California 94305, USA*
[7]*SIMES, SLAC National Accelerator Laboratory, Menlo Park, California 94025, USA*
[8]*Geballe Laboratory for Advanced Materials, Stanford University, Stanford, California 94305, USA*
[9]*Department of Materials Science and Engineering, Stanford University, Stanford, California 94305, USA*
[10]*Institute for Theoretical Physics, ETH Zurich, 8093 Zurich, Switzerland*

(Received 2 March 2021; accepted 1 October 2021; published 24 November 2021)

Engineering novel states of matter with light is at the forefront of materials research. An intensely studied direction is to realize broken-symmetry phases that are "hidden" under equilibrium conditions but can be unleashed by an ultrashort laser pulse. Despite a plethora of experimental discoveries, the nature of these orders and how they transiently appear remain unclear. To this end, we investigate a nonequilibrium charge density wave (CDW) in rare-earth tritellurides, which is suppressed in equilibrium but emerges after photoexcitation. Using a pump-pump-probe protocol implemented in ultrafast electron diffraction, we demonstrate that the light-induced CDW consists solely of order parameter fluctuations, which bear striking similarities to critical fluctuations in equilibrium despite differences in the length scale. By calculating the dynamics of CDW fluctuations in a nonperturbative model, we further show that the strength of the light-induced order is governed by the amplitude of equilibrium fluctuations. These findings highlight photoinduced fluctuations as an important ingredient for the emergence of transient orders out of equilibrium. Our results further suggest that materials with strong fluctuations in equilibrium are promising platforms to host hidden orders after laser excitation.

DOI: 10.1103/PhysRevLett.127.227401

In a symmetry-breaking phase transition, fluctuations of the order parameter provide important information about the way an ordered state develops. Near the transition temperature T_c, fluctuations exhibit a diverging correlation length and correlation time, whose critical exponents define the underlying universality class. In contrast to the equilibrium situation, the role of order parameter fluctuations remains unclear if a phase transition proceeds under nonequilibrium conditions. Of particular interest are transitions instigated by an intense laser pulse, which has led to discoveries of many hidden orders that are not accessible in thermal equilibrium, such as light-induced superconductivity [1–3], charge or spin density waves [4–7], and ferroelectricity [8,9]. These out-of-equilibrium orders are often short-lived, raising the question of whether they exist in the form of fluctuations and, if so, how they are related to fluctuations in equilibrium.

Empirically, several material classes that host transient states also display strong equilibrium fluctuations of the associated order [3,8–14]. In underdoped cuprates, where light-induced superconductivity was discovered [10–13], pronounced superconducting fluctuations are expected due to the small phase stiffness and poor screening [15]. In κ-type organic salts, where light-induced superconductivity was observed above T_c, Nernst effect measurements also pointed toward large fluctuations due to a nearby Mott criticality [3,16,17]. In cases where equilibrium fluctuations do not yield an ordered state at finite temperature, such as in the quantum paraelectric phase of $SrTiO_3$, a terahertz pulse can induce a ferroelectric state in a metastable fashion [8,9,18]. These observations suggest that photoinduced orders may be a special manifestation of equilibrium fluctuations, but experimental evidence is lacking to formally establish a link between the two entities.

Here, through a side-by-side comparison, we show that a newly discovered photoinduced charge density wave (CDW) [4,5] shares the key characteristics of the CDW fluctuations at T_c even though the former does not have a

diverging correlation length. The comparison was enabled by a pump-pump-probe scheme with ultrafast electron diffraction, which gives a direct measurement of fluctuations through diffuse scatterings. Using a nonperturbative calculation, we further demonstrate that the intensity of the photoinduced CDW peak increases with the strength of the CDW fluctuations in equilibrium. The positive correlation suggests that a photoinduced hidden state is more likely found in systems with significant equilibrium fluctuations, paving the way forward as we search for novel nonequilibrium orders.

The charge density wave is hosted by the rare-earth tritelluride ($R\mathrm{Te}_3$) family. All members possess a layered structure and the CDW instability is found in the nearly square-shaped Te sheets [Fig. 1(a)]. The quasi-two-dimensional nature of the crystals leads to a much reduced T_c compared to the mean-field transition temperature. This gives rise to significant CDW fluctuations above T_c, as evidenced by Raman spectroscopy [19] and inelastic x-ray scattering [20]. The near-C_4 symmetry of the Te sheets leads to two competing CDWs: The dominant one has a modulation along the c axis, while the subdominant one is modulated along the orthogonal a axis [21]. Here, we focus on LaTe_3 ($T_c \approx 670$ K) and DyTe_3 [$T_c = 306(3)$ K] [21,22]. They share nearly identical properties, except for the different transition temperatures [23]. Hence, under similar experimental conditions, we have access to CDW fluctuations in the critical regime near T_c (DyTe_3), as well as a state with only the dominant c-axis CDW (LaTe_3).

Figures 1(d) and 1(e) show the equilibrium electron diffraction patterns of DyTe_3 in the $(H, 0, L)$ plane, taken below and near T_c (see Supplemental Material [25] for experimental details). At 100 K, pairs of CDW satellite peaks are found along the c axis at a wave vector $q_c = 0.294(1)c^*$ (blue arrows), but no satellite peaks are observed along the orthogonal a axis [62]. When the sample is heated to T_c, the c-axis peaks significantly weaken but remain visible [Fig. 1(e)]; in the meantime, diffuse spots arise along the a axis (red arrows). Notably, the diffraction pattern appears symmetric between the c and a axis, as highlighted by three observations: (i) brighter $(H \pm q_a, 0, L)$ satellites are found along the c axis than along the a axis, and vice versa for the $(H, 0, L \pm q_c)$ peaks; (ii) the CDW wave vectors are similar, $q_a \approx q_c$; and (iii) the satellite intensities are comparable for the two CDWs. Transverse atomic displacements associated with both CDWs account for the intensity pattern in (i) [25]. Observations (ii) and (iii) preclude the possibility of a long-range CDW along the a axis that is known to occur in DyTe_3 below 68 K $\ll T_c$ [20] because this low-temperature a-axis peak has a markedly different wave vector and a much weaker diffraction intensity compared to its c-axis counterpart [4,63]. The symmetric appearance of the diffuse spots in Fig. 1(e) is a signature unique to the critical regime near T_c. Below T_c, such symmetry is broken

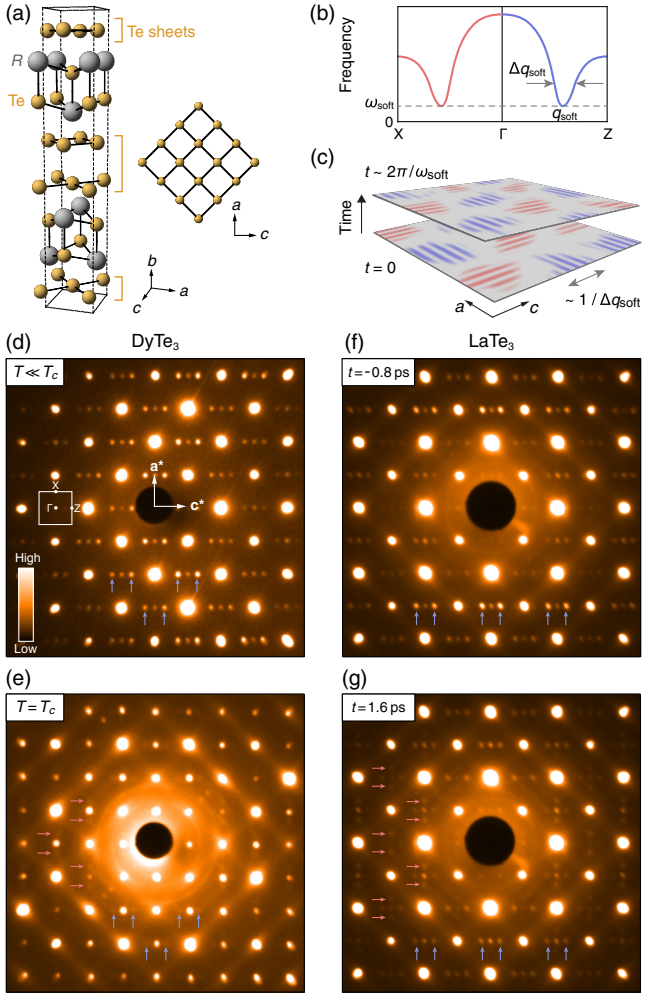

FIG. 1. Competing charge density waves in rare-earth tritellurides. (a) Left: schematic of the layered structure of $R\mathrm{Te}_3$, where dashed lines indicate the primary unit cell. Right: enlarged view of the nearly square-shaped Te sheets that host the CDW instabilities. (b) Schematic phonon dispersion right above T_c along Γ-X and Γ-Z, featuring two Kohn anomalies at q_{soft}. (c) Schematic of fluctuating CDWs right above T_c. (d),(e) Equilibrium electron diffractions of DyTe_3 [$T_c = 306(3)$ K [24]] taken at 100 K (d) and 307 K (e). (f),(g) Time-resolved diffractions of LaTe_3 (f) before and (g) 1.6 ps after photoexcitation by an 80-fs, 800-nm laser pulse with an incident fluence of 2.1 mJ/cm^2, measured at 307 K. Blue and red arrows indicate the CDW peaks along the c and a axis, respectively. Difference in intensities of lattice Bragg peaks in (d) and (e) results from slight sample drift and tilt during the warm-up process.

by the long-range c-axis CDW. At temperatures significantly exceeding T_c, fluctuations are weak, rendering any diffuse scattering invisible under the background intensity.

We now turn to LaTe_3 and study the behavior of the CDWs out of equilibrium. Figures 1(f) and 1(g) show the electron diffraction patterns taken 0.8 ps before and 1.6 ps after the incidence of an 80-fs, 800-nm laser pulse. After photoexcitation, the long-range CDW order along the c axis

is suppressed (blue arrows), while new peaks appear along the a axis (red arrows), whose intensity increases monotonically with pump laser fluence [4,25]. Remarkably, the CDW superlattice spots in this transient snapshot of the photoexcited state are visually indistinguishable from those in the equilibrium diffraction pattern recorded at T_c in $DyTe_3$ [Figs. 1(e) and 1(g)]. In particular, the transient CDW satellites along both axes share a similar intensity and wave vector, hinting at a restored symmetry between the two CDWs.

The similarity between Figs. 1(e) and 1(g) allows us to interpret the light-induced CDW state using an equilibrium picture close to T_c. In momentum space, the diffuse satellite peaks are indicative of the population of transient soft phonons along the a^* and c^* axis [Fig. 1(b)]. In real space, this critical regime is characterized by short-range CDW patches in both directions [Fig. 1(c)], with the correlation length inversely proportional to the momentum width of the Kohn anomaly [25]. From inelastic x-ray measurements [20], the phonon energies at q_a and q_c are approximately 1–2 meV, corresponding to a fluctuating timescale of 2–4 ps for these CDW patches. A similar timescale is observed as the lifetime of the light-induced a-axis CDW [Fig. S4(a) [25]]. This energy-time correspondence suggests that the light-induced a-axis CDW is indistinguishable from a soft phonon at the corresponding wave vector, confirming the intimate link between the photoexcited state and the critical regime near T_c.

The comparison between the photoexcited and the critical state suggests that the photoinduced a-axis CDW in $LaTe_3$ does not have long-range order and remains fluctuating. While the statement can be rigorously proven by simple theoretical arguments [25], here we give an estimate of the *finite* correlation length of the a-axis CDW. Based on the diffraction peak width w [Fig. 1(g)], which is limited by instrumental resolution, the correlation length has a lower bound of $1/w \sim 3.5$ nm, or eight crystallographic unit cells (u.c.). Given the approximate CDW lifetime τ of 4 ps [Fig. S4(a)], the correlation length is at most $v\tau \sim 10$ nm (23 u.c.), where $v = 2500$ m/s is the speed of sound along the a axis [64]. This upper bound is a testament that each fluctuating patch cannot establish phase coherence with its neighbors at a speed faster than phonon propagation. Compared to the correlation length of the dominant c-axis CDW in equilibrium, which is estimated to be at least 1.8 μm within Te planes [21], the particularly small value of $v\tau$ hence confirms the absence of long-range order along the a axis and suggests that the light-induced CDW consists entirely of short-range fluctuations.

An almost square-symmetric diffraction pattern after photoexcitation and at equilibrium T_c is suggestive of a close connection between the two states. To further elucidate their relationship, we investigate their response to an external perturbation. By comparing the respective dynamics of the order parameter fluctuations, we can gain some crucial insights into the similarities and differences between the two regimes. To this end, we apply a second laser pulse to $LaTe_3$ right after the emergence of the a-axis satellite peak and record the intensity evolution of the CDW fluctuations along both axes. As a reference, we also photoexcite $DyTe_3$ at its CDW transition temperature, where fluctuations of both density waves abound.

We first examine the laser-induced response in $DyTe_3$ at its T_c [Fig. 2(a)]. After photoexcitation, the diffuse satellite spots display an initial dip in intensity followed by a fast recovery, a trend perfectly mirrored in both axes [Figs. 2(e) and 2(g)]. These dynamics are in stark contrast to diffuse scattering intensities at other momenta away from Bragg or CDW peaks, where only a single-exponential rise is observed [Fig. 2(c)]. The dip can be understood in two equivalent ways. From the phonon perspective, it represents a transient stiffening of the soft mode [25,67]. As electrons are excited to high energy, there is a transient reduction in the electronic band occupation near the Fermi energy that interacts with the lattice ions. This reduction leads to an increase in the renormalized phonon frequency and hence a decrease in the phonon population, as suggested by the equipartition theorem. An alternative viewpoint is based on the classical description of phonons as atomic displacements in real space. In each frame diffracted from a single electron pulse, we capture a snapshot of the system, such as the one depicted in Fig. 1(c). The dip hence indicates a smaller lattice distortion amplitude in the fluctuating CDW patches, averaged over space and over all snapshots at the same pump-probe delay. The second perspective naturally connects the photoinduced melting of fluctuating CDWs to the melting of a long-range CDW. Locally, there is minimal distinction between the two processes and both occur over ~0.4 ps, a timescale dictated by the phonon period associated with the CDW distortion [68,69]. In Figs. 2(e) and 2(g), we observe that the intensities quickly rise after the dip, indicating an increased phonon population from laser-induced heating. After subtracting the thermal diffuse contribution, the dip only partially recovers [Fig. 2(i)], suggesting an elevated lattice temperature above T_c, where the Kohn anomaly becomes less pronounced.

Next, we study the dynamics in the photoexcited state of $LaTe_3$. As illustrated in Fig. 2(b), we use the first laser pulse to bring the material into a nonequilibrium state, where we have observed a symmetric appearance of diffuse satellite spots along both a and c axes. We then apply a second pulse to perturb this transient state and look at the response of the two competing CDW fluctuations. In the experiment, the two pump pulses share the same *incident* fluence. To assess the *absorbed* fluence, we note that the maximum value attained in thermal diffuse scattering doubles after the second pulse [Fig. 2(d)]. This observation affirms that energy absorption is minimally affected by the presence of excited carriers after the first pulse. We now

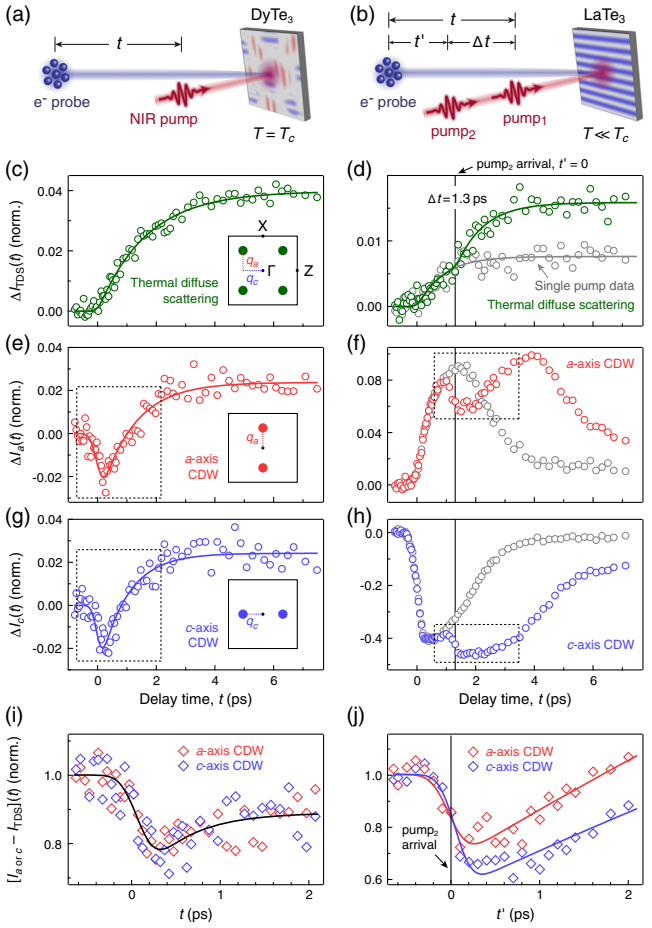

FIG. 2. Response of CDW fluctuations to photoexcitation. (a), (b) Schematic setups for $DyTe_3$ and $LaTe_3$. Both samples were kept at $T = 307$ K. The incident fluence was 3.3 mJ/cm^2 in (a) and 1.0 mJ/cm^2 for each pump in (b). (c)–(h) Changes in the integrated intensities for thermal diffuse scattering [I_{TDS}, (c),(d)], a-axis CDW peak [I_a, (e),(f)], and c-axis CDW peak [I_c, (g),(h)]. Integration areas are marked by solid circles in the insets. Traces are normalized by the average value of I_c before photoexcitation. In (d),(f),(h), vertical lines indicate the arrival time of pump$_2$ at $\Delta t = 1.3$ ps. For reference, dynamics in the absence of pump$_2$ is shown in gray. (i),(j) Enlarged view of dashed rectangles in (e)–(h) after subtracting the respective thermal diffuse background [I_{TDS} in (c),(d)]. In (i), traces are normalized by the average values at $t < 0$. In (j), traces are plotted as a function of the relative delay between the probe pulse and pump$_2$ (t'), where intensities are normalized by the average value in the interval $t' \in [-0.7, -0.2]$ ps. A slightly larger reduction along the c axis is attributed to a mismatch between pumped and probed volumes, leading to additional melting of residual long-range CDW by the second pulse. In (c)–(j), solid curves are fits to a phenomenological model in Eq. (S1) (see Supplemental Material [25]). The black fitted curve in (i) uses the averaged data along the a and c axes.

move on to analyze the CDW peaks, shown in Figs. 2(f) and 2(h). Unlike their distinct behavior upon the initial photoexcitation, the intensity evolution of the peaks along both axes share almost identical trends after the second pulse. For a direct comparison between the two orders, we examine their dynamics right after the second pulse and plot them together in Fig. 2(j), where intensities from thermal diffuse scattering have been subtracted using the same procedure applied to $DyTe_3$. Similar to the fluctuating CDWs in $DyTe_3$ near T_c, the two diffuse peaks in $LaTe_3$ feature a transient reduction in the fluctuation amplitude, followed by a recovery that lasts for more than 2 ps. Unlike $DyTe_3$, the satellite intensities in $LaTe_3$ are fully recovered compared to their values just before the second pulse, suggesting the nonthermal nature of these density wave fluctuations.

The similarities between the excited state in $LaTe_3$ and the critical state in $DyTe_3$—both in their diffraction snapshots (Fig. 1) and in their photoinduced dynamics (Fig. 2)—suggest that the light-induced CDW is a special manifestation of critical fluctuations. While the equilibrium fluctuations near T_c are thermal and follow the scaling relations prescribed by the theory of renormalization group [70], the light-induced fluctuations may not conform to a thermodynamic distribution [71]. To understand how the strength of equilibrium fluctuations affects the appearance of the light-induced CDW, we developed a time-dependent Ginzburg-Landau formalism within the Gaussian approximation (see Supplemental Material [25] for derivation). This approach gives a nonperturbative solution to the light-induced dynamics, yielding quantities that have a one-to-one correspondence to the observables in our time-resolved diffraction experiments. Unlike N-temperature models [72], here we do not need to artificially assign a temperature to each degree of freedom in the system.

To assess the validity of the model, we first calculate intensity evolution of a- and c-axis CDW peaks after photoexcitation [Fig. 3(a)]. The simulated trends

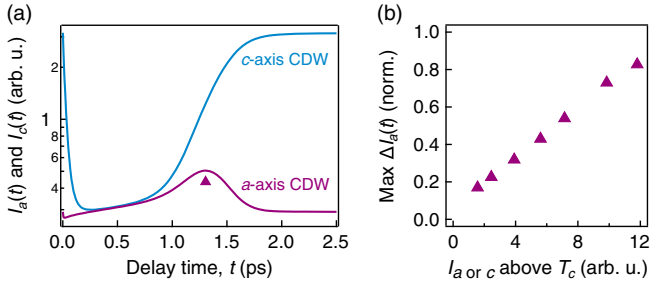

FIG. 3. Simulated dynamics of photoinduced CDW and its relation to equilibrium fluctuations. (a) Evolution of integrated intensities of the c- (blue) and a-axis (red) CDW peak upon photoexciting the unidirectional CDW state. Triangle marks the maximum intensity of the light-induced CDW. The nonzero value of the a-axis peak at $t = 0$ originates from thermal fluctuations. (b) Maximum intensity change of the photoinduced a-axis CDW peak [$\Delta I_a(t)$] as a function of equilibrium diffuse intensity at a fixed temperature above T_c, the latter of which quantifies thermal fluctuations and is indistinguishable between the two axes. $\Delta I_a(t)$ is normalized by $I_a(t = 0)$ (see Fig. S8 [25]).

successfully reproduce the experimental observations (Fig. S4 [25]). The transient enhancement of intensity along the a axis is solely the result of CDW fluctuations without long-range order [25]. In Fig. 3(b), as we reduce the order parameter stiffness to increase the amplitude of equilibrium fluctuations above T_c, the strength of the transient CDW order also increases under identical photoexcitation conditions. This positive correlation suggests that strong fluctuations in equilibrium constitute an important factor for observing light-induced ordering phenomena out of equilibrium.

Despite the similarities between the light-induced CDW and the critical fluctuations, there exist important differences (see Supplemental Material [25]). For example, the transient lattice temperature of $LaTe_3$ stays far below its equilibrium T_c, and there is no change in the in-plane lattice anisotropy after photoexcitation, distinct from the evolution of a and c lattice parameters across T_c [4,21]. Importantly, the light-induced CDW has a finite correlation length for all time delays, but at the critical point in equilibrium, correlation length diverges with fluctuations occurring at all length scales. Hence, strictly speaking, the photoexcited state is not truly critical as described in a thermodynamic transition.

By leveraging the symmetry between two competing CDWs in RTe_3, we have elicited the correspondence between a photoinduced order and critical fluctuations in equilibrium. The parallels provide a nonthermal pathway to access hidden symmetries of a system even if T_c is unattainable under equilibrium condition. The similarities also hint at the existence of universal scaling laws that govern the dynamics of a highly nonequilibrium system [71], which have been detected in scattering experiments with high momentum resolution and an extended time delay [73–75]. Furthermore, our results offer a generic mechanism for the creation of photoinduced states, which can emerge as order parameter fluctuations in the absence of long-range order. This insight suggests that one should look for material classes that exhibit strong order parameter fluctuations in equilibrium in order to look for hidden states out of equilibrium. Experimental signatures for such strong fluctuations depend on the order parameter, ranging from diffuse peaks in a charge or spin density wave system to Nernst effect in a superconductor [25]. We expect the connection between equilibrium fluctuations and out-of-equilibrium ordering to hold regardless of microscopic details, providing a guiding principle in our search for other light-induced states.

We thank Mariano Trigo and Yu He for helpful discussions. This work was mainly funded by the U.S. Department of Energy, BES DMSE (data taking and analysis) and the Gordon and Betty Moore Foundation's EPiQS Initiative Grant No. GBMF9459 (modeling and manuscript writing). We acknowledge support from the U.S. Department of Energy BES SUF Division Accelerator and Detector R&D program, the LCLS Facility, and SLAC under Awards No. DE-AC02-05-CH11231 and No. DE-AC02-76SF00515 (MeV UED at SLAC). Sample growth and characterization work at Stanford was supported by the U.S. Department of Energy, Office of Basic Energy Sciences, under Award No. DEAC02-76SF00515. A. Z. acknowledges support from the Miller Institute for Basic Research in Science. This research was partly supported by the Army Research Office through Grant No. W911NF1810316, and the Gordon and Betty Moore Foundation EPiQS Initiative through Grant No. GBMF9643 to P. J.-H. (sample preparation and characterization). This work made use of the Materials Research Science and Engineering Center shared experimental facilities supported by the National Science Foundation (NSF) (Grant No. DMR-0819762). This work was performed in part at the Harvard University Center for Nanoscale Systems (CNS), a member of the National Nanotechnology Coordinated Infrastructure Network (NNCI), which is supported by the National Science Foundation under NSF ECCS Grant No. 1541959. P. E. D. and E. D. were supported by Harvard-MIT CUA, AFOSR-MURI: Photonic Quantum Matter Grant No. FA95501610323, Harvard Quantum Initiative.

*These authors contributed equally to this work.
†Corresponding author.
gedik@mit.edu

[1] S. Kaiser, Light-induced superconductivity in high-T_c cuprates, Phys. Scr. **92**, 103001 (2017).
[2] M. Mitrano, A. Cantaluppi, D. Nicoletti, S. Kaiser, A. Perucchi, S. Lupi, P. Di Pietro, D. Pontiroli, M. Riccò, S. R. Clark, D. Jaksch, and A. Cavalleri, Possible light-induced superconductivity in K_3C_{60} at high temperature, Nature (London) **530**, 461 (2016).
[3] M. Buzzi *et al.*, Photomolecular High-Temperature Superconductivity, Phys. Rev. X **10**, 031028 (2020).
[4] A. Kogar *et al.*, Light-induced charge density wave in $LaTe_3$, Nat. Phys. **16**, 159 (2020).
[5] F. Zhou, J. Williams, S. Sun, C. D. Malliakas, M. G. Kanatzidis, A. F. Kemper, and C.-Y. Ruan, Nonequilibrium dynamics of spontaneous symmetry breaking into a hidden state of charge-density wave, Nat. Commun. **12**, 566 (2021).
[6] T.-R. T. Han, F. Zhou, C. D. Malliakas, P. M. Duxbury, S. D. Mahanti, M. G. Kanatzidis, and C.-Y. Ruan, Exploration of metastability and hidden phases in correlated electron crystals visualized by femtosecond optical doping and electron crystallography, Sci. Adv. **1**, e1400173 (2015).
[7] K. W. Kim, A. Pashkin, H. Schäfer, M. Beyer, M. Porer, T. Wolf, C. Bernhard, J. Demsar, R. Huber, and A. Leitenstorfer, Ultrafast transient generation of spin-density-wave order in the normal state of $BaFe_2As_2$ driven by coherent lattice vibrations, Nat. Mater. **11**, 497 (2012).
[8] X. Li, T. Qiu, J. Zhang, E. Baldini, J. Lu, A. M. Rappe, and K. A. Nelson, Terahertz field-induced ferroelectricity in quantum paraelectric $SrTiO_3$, Science **364**, 1079 (2019).

[9] T. F. Nova, A. S. Disa, M. Fechner, and A. Cavalleri, Metastable ferroelectricity in optically strained $SrTiO_3$, Science **364**, 1075 (2019).
[10] D. Fausti, R. I. Tobey, N. Dean, S. Kaiser, A. Dienst, M. C. Hoffmann, S. Pyon, T. Takayama, H. Takagi, and A. Cavalleri, Light-induced superconductivity in a stripe-ordered cuprate, Science **331**, 189 (2011).
[11] S. Kaiser, C. R. Hunt, D. Nicoletti, W. Hu, I. Gierz, H. Y. Liu, M. Le Tacon, T. Loew, D. Haug, B. Keimer, and A. Cavalleri, Optically induced coherent transport far above T_c in underdoped $YBa_2Cu_3O_{6+\delta}$, Phys. Rev. B **89**, 184516 (2014).
[12] W. Hu, S. Kaiser, D. Nicoletti, C. R. Hunt, I. Gierz, M. C. Hoffmann, M. Le Tacon, T. Loew, B. Keimer, and A. Cavalleri, Optically enhanced coherent transport in $YBa_2Cu_3O_{6.5}$ by ultrafast redistribution of interlayer coupling, Nat. Mater. **13**, 705 (2014).
[13] D. Nicoletti, E. Casandruc, Y. Laplace, V. Khanna, C. R. Hunt, S. Kaiser, S. S. Dhesi, G. D. Gu, J. P. Hill, and A. Cavalleri, Optically induced superconductivity in striped $La_{2-x}Ba_xCuO_4$ by polarization-selective excitation in the near infrared, Phys. Rev. B **90**, 100503(R) (2014).
[14] S. Borroni, E. Baldini, V. M. Katukuri, A. Mann, K. Parlinski, D. Legut, C. Arrell, F. van Mourik, J. Teyssier, A. Kozlowski, P. Piekarz, O. V. Yazyev, A. M. Oleś, J. Lorenzana, and F. Carbone, Coherent generation of symmetry-forbidden phonons by light-induced electron-phonon interactions in magnetite, Phys. Rev. B **96**, 104308 (2017).
[15] V. J. Emery and S. A. Kivelson, Importance of phase fluctuations in superconductors with small superfluid density, Nature (London) **374**, 434 (1995).
[16] M.-S. Nam, A. Ardavan, S. J. Blundell, and J. A. Schlueter, Fluctuating superconductivity in organic molecular metals close to the Mott transition, Nature (London) **449**, 584 (2007).
[17] F. Kagawa, K. Miyagawa, and K. Kanoda, Magnetic Mott criticality in a κ-type organic salt probed by NMR, Nat. Phys. **5**, 880 (2009).
[18] K. A. Müller and H. Burkard, $SrTiO_3$: An intrinsic quantum paraelectric below 4 K, Phys. Rev. B **19**, 3593 (1979).
[19] H.-M. Eiter, M. Lavagnini, R. Hackl, E. A. Nowadnick, A. F. Kemper, T. P. Devereaux, J.-H. Chu, J. G. Analytis, I. R. Fisher, and L. Degiorgi, Alternative route to charge density wave formation in multiband systems, Proc. Natl. Acad. Sci. U.S.A. **110**, 64 (2013).
[20] M. Maschek, D. A. Zocco, S. Rosenkranz, R. Heid, A. H. Said, A. Alatas, P. Walmsley, I. R. Fisher, and F. Weber, Competing soft phonon modes at the charge-density-wave transitions in $DyTe_3$, Phys. Rev. B **98**, 094304 (2018).
[21] N. Ru, C. L. Condron, G. Y. Margulis, K. Y. Shin, J. Laverock, S. B. Dugdale, M. F. Toney, and I. R. Fisher, Effect of chemical pressure on the charge density wave transition in rare-earth tritellurides RTe_3, Phys. Rev. B **77**, 035114 (2008).
[22] B. F. Hu, B. Cheng, R. H. Yuan, T. Dong, and N. L. Wang, Coexistence and competition of multiple charge-density-wave orders in rare-earth tritellurides, Phys. Rev. B **90**, 085105 (2014).
[23] Unlike $LaTe_3$ that only develops a unidirectional CDW under ambient pressure, there are two CDW transitions in $DyTe_3$ [24]. Starting from its normal metallic state, $DyTe_3$ first develops a unidirectional CDW at T_{c1}; the second transition into a bidirectional CDW state occurs at a lower temperature T_{c2}. Here, we are only concerned with the high-temperature transition and we denote T_{c1} by T_c for brevity.
[24] N. Ru, Charge density wave formation in rare-earth tellurides, Ph.D. thesis, Stanford University, Stanford 2008, https://web.stanford.edu/group/fisher/people/Nancy_Ru_thesis.pdf.
[25] See Supplemental Material at http://link.aps.org/supplemental/10.1103/PhysRevLett.127.227401 for additional details of the experimental setups, analysis procedures, theoretical formalism, and further discussions. It includes 11 sections: (i) experimental details, (ii) diffraction intensity near a Kohn anomaly, (iii) transverse atomic displacement and Bragg peak dynamics, (iv) momentum-dependent diffuse scattering dynamics, (v) initial CDW dynamics after photoexcitation, (vi) fluence-dependent slowing down in the fluctuation dynamics, (vii) nonperturbative calculation of photoinduced fluctuations, (viii) fluctuations in the dominant CDW, (ix) comparison of photoexcited and critical states, (x) experimental indicators of order parameter fluctuations, and (xi) underlying high-energy symmetries revealed by photoexcitation. The Supplemental Material includes Refs. [26–61].
[26] N. Ru and I. R. Fisher, Thermodynamic and transport properties of YTe_3, $LaTe_3$, $CeTe_3$, Phys. Rev. B **73**, 033101 (2006).
[27] Y.-Q. Bie, A. Zong, X. Wang, P. Jarillo-Herrero, and N. Gedik, A versatile sample fabrication method for ultrafast electron diffraction, Ultramicroscopy **230**, 113389 (2021).
[28] S. P. Weathersby *et al.*, Mega-electron-volt ultrafast electron diffraction at SLAC National Accelerator Laboratory, Rev. Sci. Instrum. **86**, 073702 (2015).
[29] X. Shen, R. K. Li, U. Lundström, T. J. Lane, A. H. Reid, S. P. Weathersby, and X. J. Wang, Femtosecond mega-electron-volt electron microdiffraction, Ultramicroscopy **184**, 172 (2018).
[30] R. G. Moore *et al.*, Ultrafast resonant soft x-ray diffraction dynamics of the charge density wave in $TbTe_3$, Phys. Rev. B **93**, 024304 (2016).
[31] A. Sacchetti, L. Degiorgi, T. Giamarchi, N. Ru, and I. R. Fisher, Chemical pressure and hidden one-dimensional behavior in rare-earth tri-telluride charge-density wave compounds, Phys. Rev. B **74**, 125115 (2006).
[32] T. H. Ramsey, H. Steinfink, and E. J. Weiss, Thermoelectric and electrical measurements in the La-Te System, J. Appl. Phys. **36**, 548 (1965).
[33] L. P. René de Cotret, J.-H. Pöhls, M. J. Stern, M. R. Otto, M. Sutton, and B. J. Siwick, Time- and momentum-resolved phonon population dynamics with ultrafast electron diffuse scattering, Phys. Rev. B **100**, 214115 (2019).
[34] M. Maschek, S. Rosenkranz, R. Heid, A. H. Said, P. Giraldo-Gallo, I. R. Fisher, and F. Weber, Wave-vector-dependent electron-phonon coupling and the charge-density-wave transition in $TbTe_3$, Phys. Rev. B **91**, 235146 (2015).
[35] M. J. Stern, L. P. René de Cotret, M. R. Otto, R. P. Chatelain, J.-P. Boisvert, M. Sutton, and B. J. Siwick, Mapping momentum-dependent electron-phonon coupling and

nonequilibrium phonon dynamics with ultrafast electron diffuse scattering, Phys. Rev. B **97**, 165416 (2018).
[36] G. F. Mazenko and M. Zannetti, Instability, spinodal decomposition, and nucleation in a system with continuous symmetry, Phys. Rev. B **32**, 4565 (1985).
[37] A. J. Bray, Theory of phase-ordering kinetics, Adv. Phys. **43**, 357 (1994).
[38] A. Zong, A. Kogar, Y.-Q. Bie, T. Rohwer, C. Lee, E. Baldini, E. Ergeçen, M. B. Yilmaz, B. Freelon, E. J. Sie, H. Zhou, J. Straquadine, P. Walmsley, P. E. Dolgirev, A. V. Rozhkov, I. R. Fisher, P. Jarillo-Herrero, B. V. Fine, and N. Gedik, Evidence for topological defects in a photoinduced phase transition, Nat. Phys. **15**, 27 (2019).
[39] P. M. Chaikin and T. C. Lubensky, Mean-field theory, in *Principles of Condensed Matter Physics* (Cambridge University Press, Cambridge, England, 1995), pp. 144–212.
[40] P. C. Hohenberg and B. I. Halperin, Theory of dynamic critical phenomena, Rev. Mod. Phys. **49**, 435 (1977).
[41] Z. Sun and A. J. Millis, Transient Trapping into Metastable States in Systems with Competing Orders, Phys. Rev. X **10**, 021028 (2020).
[42] M. Trigo, P. Giraldo-Gallo, M. E. Kozina, T. Henighan, M. P. Jiang, H. Liu, J. N. Clark, M. Chollet, J. M. Glownia, D. Zhu, T. Katayama, D. Leuenberger, P. S. Kirchmann, I. R. Fisher, Z. X. Shen, and D. A. Reis, Coherent order parameter dynamics in $SmTe_3$, Phys. Rev. B **99**, 104111 (2019).
[43] M. Holt, P. Zschack, H. Hong, M. Y. Chou, and T.-C. Chiang, X-Ray Studies of Phonon Softening in $TiSe_2$, Phys. Rev. Lett. **86**, 3799 (2001).
[44] R. M. Glaeser, Electron crystallography of biological macromolecules, Annu. Rev. Phys. Chem. **36**, 243 (1985).
[45] L. Rettig, R. Cortés, J.-H. Chu, I. R. Fisher, F. Schmitt, R. G. Moore, Z.-X. Shen, P. S. Kirchmann, M. Wolf, and U. Bovensiepen, Persistent order due to transiently enhanced nesting in an electronically excited charge density wave, Nat. Commun. **7**, 10459 (2016).
[46] T. Yokoya, T. Kiss, A. Chainani, S. Shin, and K. Yamaya, Role of charge-density-wave fluctuations on the spectral function in a metallic charge-density-wave system, Phys. Rev. B **71**, 140504(R) (2005).
[47] U. Chatterjee, J. Zhao, M. Iavarone, R. Di Capua, J. P. Castellan, G. Karapetrov, C. D. Malliakas, M. G. Kanatzidis, H. Claus, J. P. C. Ruff, F. Weber, J. van Wezel, J. C. Campuzano, R. Osborn, M. Randeria, N. Trivedi, M. R. Norman, and S. Rosenkranz, Emergence of coherence in the charge-density wave state of $2H$-$NbSe_2$, Nat. Commun. **6**, 6313 (2015).
[48] Z. A. Xu, N. P. Ong, Y. Wang, T. Kakeshita, and S. Uchida, Vortex-like excitations and the onset of superconducting phase fluctuation in underdoped $La_{2-x}Sr_xCuO_4$, Nature (London) **406**, 486 (2000).
[49] A. Pourret, H. Aubin, J. Lesueur, C. A. Marrache-Kikuchi, L. Bergé, L. Dumoulin, and K. Behnia, Observation of the Nernst signal generated by fluctuating Cooper pairs, Nat. Phys. **2**, 683 (2006).
[50] M.-S. Nam, C. Mézière, P. Batail, L. Zorina, S. Simonov, and A. Ardavan, Superconducting fluctuations in organic molecular metals enhanced by Mott criticality, Sci. Rep. **3**, 3390 (2013).
[51] M. Buzzi, D. Nicoletti, S. Fava, G. Jotzu, K. Miyagawa, K. Kanoda, A. Henderson, T. Siegrist, J. A. Schlueter, M.-S. Nam, A. Ardavan, and A. Cavalleri, A Phase Diagram for Light-Induced Superconductivity in κ-$(ET)_2$-X, arXiv:2106.14244 [Phys. Rev. Lett. (to be published)].
[52] Y. He, S.-D. Chen, Z.-X. Li, D. Zhao, D. Song, Y. Yoshida, H. Eisaki, T. Wu, X.-H. Chen, D.-H. Lu, C. Meingast, T. P. Devereaux, R. J. Birgeneau, M. Hashimoto, D.-H. Lee, and Z.-X. Shen, Superconducting Fluctuations in Overdoped $Bi_2Sr_2CaCu_2O_{8+\delta}$, Phys. Rev. X **11**, 031068 (2021).
[53] J. L. Tallon, J. G. Storey, and J. W. Loram, Fluctuations and critical temperature reduction in cuprate superconductors, Phys. Rev. B **83**, 092502 (2011).
[54] F. Weber, S. Rosenkranz, J.-P. Castellan, R. Osborn, R. Hott, R. Heid, K.-P. Bohnen, T. Egami, A. H. Said, and D. Reznik, Extended Phonon Collapse and the Origin of the Charge-Density Wave in $2H$-$NbSe_2$, Phys. Rev. Lett. **107**, 107403 (2011).
[55] M. Hoesch, A. Bosak, D. Chernyshov, H. Berger, and M. Krisch, Giant Kohn Anomaly and the Phase Transition in Charge Density Wave $ZrTe_3$, Phys. Rev. Lett. **102**, 086402 (2009).
[56] G. Grüner, *Density Waves in Solids* (Addison-Wesley, Boston, 1994).
[57] L. Ma and W.-Q. Yu, Review of nuclear magnetic resonance studies on iron-based superconductors, Chin. Phys. B **22**, 087414 (2013).
[58] J. Zhang, X. Tan, M. Liu, S. W. Teitelbaum, K. W. Post, F. Jin, K. A. Nelson, D. N. Basov, W. Wu, and R. D. Averitt, Cooperative photoinduced metastable phase control in strained manganite films, Nat. Mater. **15**, 956 (2016).
[59] A. S. McLeod, J. Zhang, M. Q. Gu, F. Jin, G. Zhang, K. W. Post, X. G. Zhao, A. J. Millis, W. B. Wu, J. M. Rondinelli, R. D. Averitt, and D. N. Basov, Multi-messenger nanoprobes of hidden magnetism in a strained manganite, Nat. Mater. **19**, 397 (2020).
[60] S.-C. Zhang, A unified theory based on $SO(5)$ symmetry of superconductivity and antiferromagnetism, Science **275**, 1089 (1997).
[61] E. Demler, W. Hanke, and S.-C. Zhang, $SO(5)$ theory of antiferromagnetism and superconductivity, Rev. Mod. Phys. **76**, 909 (2004).
[62] The image was taken above $T_{c2} = 68$ K for $DyTe_3$ [20].
[63] J. A. W. Straquadine, F. Weber, S. Rosenkranz, A. H. Said, and I. R. Fisher, Suppression of charge density wave order by disorder in Pd-intercalated $ErTe_3$, Phys. Rev. B **99**, 235138 (2019).
[64] The speed of sound is deduced from the phonon dispersion in $DyTe_3$ calculated by density functional perturbation theory and verified by inelastic x-ray scattering [20]. The speed of sound associated with the phason excitation may be an alternative choice for this correlation length estimate. The phason dispersion is unavailable for RTe_3 but we take note of values in other incommensurate CDWs. The phason speed ranges from 4×10^2 m/s in $1T$-TaS_2 [65] to 2×10^4 m/s in $K_{0.3}MoO_3$ [66], hence not changing the conclusion that the largest possible correlation length of the transient CDW in $LaTe_3$ is still orders of magnitude smaller compared to its dominant CDW in equilibrium.

[65] W. Minor, L. D. Chapman, S. N. Ehrlich, and R. Colella, Phason velocities in TaS_2 by x-ray diffuse scattering, Phys. Rev. B **39**, 1360 (1989).

[66] J. P. Pouget, B. Hennion, C. Escribe-Filippini, and M. Sato, Neutron-scattering investigations of the Kohn anomaly and of the phase and amplitude charge-density-wave excitations of the blue bronze $K_{0.3}MoO_3$, Phys. Rev. B **43**, 8421 (1991).

[67] M. R. Otto, J.-H. Pöhls, L. P. René de Cotret, M. J. Stern, M. Sutton, and B. J. Siwick, Mechanisms of electron-phonon coupling unraveled in momentum and time: The case of soft phonons in $TiSe_2$, Sci. Adv. **7**, eabf2810 (2021).

[68] S. Hellmann, T. Rohwer, M. Kalläne, K. Hanff, C. Sohrt, A. Stange, A. Carr, M. M. Murnane, H. C. Kapteyn, L. Kipp, M. Bauer, and K. Rossnagel, Time-domain classification of charge-density-wave insulators, Nat. Commun. **3**, 1069 (2012).

[69] A. Zong *et al.*, Dynamical Slowing-Down in an Ultrafast Photoinduced Phase Transition, Phys. Rev. Lett. **123**, 097601 (2019).

[70] N. Goldenfeld, *Lectures on Phase Transitions and the Renormalization Group* (Westview, Boulder, 1992).

[71] P. E. Dolgirev, M. H. Michael, A. Zong, N. Gedik, and E. Demler, Self-similar dynamics of order parameter fluctuations in pump-probe experiments, Phys. Rev. B **101**, 174306 (2020).

[72] P. E. Dolgirev, A. V. Rozhkov, A. Zong, A. Kogar, N. Gedik, and B. V. Fine, Amplitude dynamics of charge density wave in $LaTe_3$: Theoretical description of pump-probe experiments, Phys. Rev. B **101**, 054203 (2020).

[73] C. Laulhé *et al.*, Ultrafast Formation of a Charge Density Wave State in $1T$-TaS_2: Observation at Nanometer Scales Using Time-Resolved X-Ray Diffraction, Phys. Rev. Lett. **118**, 247401 (2017).

[74] S. Vogelgesang, G. Storeck, J. G. Horstmann, T. Diekmann, M. Sivis, S. Schramm, K. Rossnagel, S. Schäfer, and C. Ropers, Phase ordering of charge density waves traced by ultrafast low-energy electron diffraction, Nat. Phys. **14**, 184 (2018).

[75] M. Mitrano, S. Lee, A. A. Husain, L. Delacretaz, M. Zhu, G. de la Peña Munoz, S. X.-L. Sun, Y. I. Joe, A. H. Reid, S. F. Wandel, G. Coslovich, W. Schlotter, T. van Driel, J. Schneeloch, G. D. Gu, S. Hartnoll, N. Goldenfeld, and P. Abbamonte, Ultrafast time-resolved x-ray scattering reveals diffusive charge order dynamics in $La_{2-x}Ba_xCuO_4$, Sci. Adv. **5**, eaax3346 (2019).